wave Theory Tech., vol. MTT-8, pp. 328–329, May 1960.
[8] M. Maeda, "An analysis of gap in microstrip transmission lines," *IEEE Trans. Microwave Theory Tech.*, vol. MTT-20, pp. 390–396, June 1972.
[9] P. Silvester and P. Benedek, "Equivalent capacitances of microstrip open circuit," *IEEE Trans. Microwave Theory Tech.*, vol. MTT-20, pp. 511–516, Aug. 1972.
[10] D. S. James and S. H. Tse, "Microstrip end effects," *Electron. Lett.*, vol. 8, pp. 46–47, Jan. 1972.
[11] J. S. Hornsby, "Full wave analysis of microstrip resonators and open-circuit end effects," *Proc. Inst. Elec. Eng., Microwaves, Optics and Antennas*, part H, vol. 129, pp. 338–341, Dec. 1982.
[12] R. H. Jansen, "Hybrid mode analysis of end effects of planar microwave and millimeter-wave transmission lines," *Proc. Inst. Elec. Eng., Microwaves, Optics and Antennas*, part H, vol. 128, pp. 77–86, Apr. 1981.
[13] L. S. Napoli and J. J. Hughes, "Foreshortening of microstrip open-circuit on alumina substrates," *IEEE Trans. Microwave Theory Tech.*, vol. MTT-19, pp. 559–561, June 1971.
[14] B. Easter, A. Gopinath, and I. M. Stephenson, "Theoretical and experimental methods for evaluating discontinuities in microstrip," *Radio Electron Eng.*, vol. 48, pp. 73–84, Jan./Feb. 1978.

Bharathi Bhat (SM'82) received the B.E. degree in electrical communication engineering and the M.E. degree in electronics, both with distinction, from the Indian Institute of Science, Bangalore, India, in 1963 and 1965, respectively. She continued her graduate studies at Harvard University, Cambridge, MA, and received the M.S. and Ph.D degrees from the Division of Engineering and Applied Physics in 1967 and 1971, respectively.

From 1971 to 1972, she worked as a Post-Doctoral Research Fellow in the Division of Engineering and Applied Physics, Harvard University. In 1973, she joined the Indian Institute of Technology, New Delhi, as an Assistant Professor. Since 1977, she has been a Professor at the Centre for Applied Research in Electronics (CARE). During the period 1979–1982, she was the Head of CARE, IIT, New Delhi. She is also the leader of the Microwave Group in CARE, and has been directing a number of sponsored research projects in the areas of microwave antennas, electronic phase shifters, and microwave and millimeter-wave integrated circuits and components.

Dr. Bhat is a Fellow of the Institution of Electronics and Telecommunication Engineers (IETE), India. She has been the Honorary Editor of the IETE Journal (electromagnetics section) since January 1981, and a member of the IETE Council since January 1982. She is presently the Chairman of the ED/MTT Chapter of the IEEE India Council.

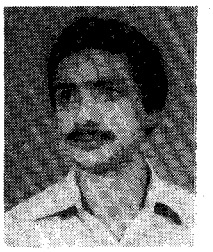

Shiban Kishen Koul (S'81–M'83) received the Bachelor of Engineering degree in electrical engineering from the Regional Engineering College, Srinagar, J&K, India, in 1977, and the Master of Technology degree in radar and communications engineering, with distinction, from the Indian Institute of Technology (IIT), Delhi, India, in 1979.

From 1979 to 1980, he worked as a Senior Research Assistant in the Centre for Applied Research in Electronics (CARE) at the Indian Institute of Technology, Delhi. Since 1980, he has been a Senior Scientific Officer in CARE. He entered the Ph.D program as a part-time student, in January 1980, and has recently received the Ph.D degree. He is presently engaged in research in the areas of thin-film microwave integrated circuits, microstrip-like transmission lines, ferrite phase shifters, and millimeter-wave transmission lines.

Multiconductor Transmission Lines in Multilayered Dielectric Media

CAO WEI, ROGER F. HARRINGTON, FELLOW, IEEE, JOSEPH R. MAUTZ, SENIOR MEMBER, IEEE, AND TAPAN K. SARKAR, SENIOR MEMBER, IEEE

***Abstract*—A method for computing the capacitance matrix and inductance matrix for a multiconductor transmission line in a multilayered dielectric region is presented. The number of conductors and the number of dielectric layers are arbitrary. Some of the conductors may be of finite cross section and others may be infinitesimally thin. The conductors are either above a single ground plane or between two parallel ground planes. The formulation is obtained by using a free-space Green's function in conjunction with total charge on the conductor-to-dielectric interfaces and polarization charge on the dielectric-to-dielectric interfaces. The solution is effected by the method of moments using pulses for expansion and point matching for testing. Computed results are given for some cases where all conducting lines are of finite cross section and other cases where they are infinitesimally thin.**

Manuscript received September 26, 1983; revised November 7, 1983. This work was supported in part by the Digital Equipment Corporation, Marlboro, MA.

C. Wei is a Visiting Scientist at Syracuse University, on leave from the Nanjing Institute of Posts and Telecommunications, China.

R. F. Harrington and J. R. Mautz are with the Department of Electrical and Computer Engineering, Syracuse University, Syracuse, NY 13210.

T. K. Sarkar is with the Department of Electrical Engineering, Rochester Institute of Technology, Rochester, NY 14623.

I. INTRODUCTION

THE OBJECTIVE of this analysis is to determine the capacitance matrix and the inductance matrix of a multiconductor transmission-line system. Some of the con-

0018-9480/84/0400-0439$01.00 ©1984 IEEE

ductors may be of finite cross section. Others may be infinitesimally thin. All of them are embedded in a multilayered dielectric material that is either above a single ground plane or contained between two ground planes. Each dielectric-to-dielectric interface is parallel to the ground plane(s).

Multiconductor transmission lines in multilayered media have been investigated by means of Green's function techniques [1]–[11], conformal mapping [12], [13], a variational method [14], a Fourier transform method [15], a Fourier integral method [16], and a generalized spectral domain analysis [17], [18]. In [3] and [11], the problem of multiconductor transmission lines in two dielectric layers is approached by using a Green's function obtained from image theory. For a two-layered dielectric, this Green's function consists of four expressions, each containing an infinite series of images. The extension of this type of Green's function to three dielectric layers consists of nine expressions, each containing a doubly infinite series of images [8]. The extension of this type of Green's function to more than three dielectric layers is impractical because, for N dielectric layers, it would consist of N^2 expressions, each containing $N-1$ infinite series.

Taking an alternative approach, the present paper uses a free-space Green's function in conjunction with total charge on the conductor-to-dielectric interfaces and polarization charge on the dielectric-to-dielectric interfaces. This approach is similar to the one in [10]. The free-space Green's function approach results in a simpler formulation of the problem, but requires the solution of a larger matrix equation. This formulation has the advantage that there is no theoretical limit to the number of dielectric layers that can be treated, but a practical limit is imposed by the speed and storage of the computer. For computational reasons, the transverse width of the dielectric layers is taken to be finite instead of infinite. If the upper ground plane is present, its width is also taken to be finite.

II. Statement of the Problem

Consider a system of multiconductor transmission lines in a multilayered dielectric region above a ground plane as shown in either Fig. 1 or Fig. 2. The system is uniform in the direction perpendicular to the xy plane. An arbitrary number N_c of perfect conductors are embedded in an arbitrary number N_d of dielectric layers. Some of the conductors may be of finite cross section. Others may be infinitesimally thin strips that appear as curves in the xy plane. The permittivity of the jth dielectric layer is ϵ_j. In Fig. 1, the uppermost dielectric extends to $y=\infty$. In Fig. 2, there is an upper ground plane.

A lower ground plane is present in both Figs. 1 and 2. This lower ground plane extends from $x=-\infty$ to $x=\infty$. Nominally, the upper ground plane and the dielectric layers also extend from $x=-\infty$ to $x=\infty$. However, the numerical solution of Section IV is obtained by truncating the upper ground plane and the dielectric layers at a finite negative value of x and a finite positive value of x.

The objective is to determine the capacitance matrix and the inductance matrix of the multiconductor transmission-line system. The ijth element of the capacitance matrix is the free charge per unit length of surface on the ith conductor when the potential of the jth conductor is one volt and the other conductors are grounded. In [3], the elements of the capacitance matrix are called coefficients of capacitance. In [19, p. 97], the diagonal elements of the capacitance matrix are called coefficients of capacitance, but the off-diagonal elements are called coefficients of induction. The inductance matrix is the product of $(\mu_0\epsilon_0)$ with the inverse of the capacitance matrix that would exist if the multilayered dielectric material were replaced by free space [20, eq. (2.24)]. Here, μ_0 is the permeability of free space, and ϵ_0 is the permittivity of free space.

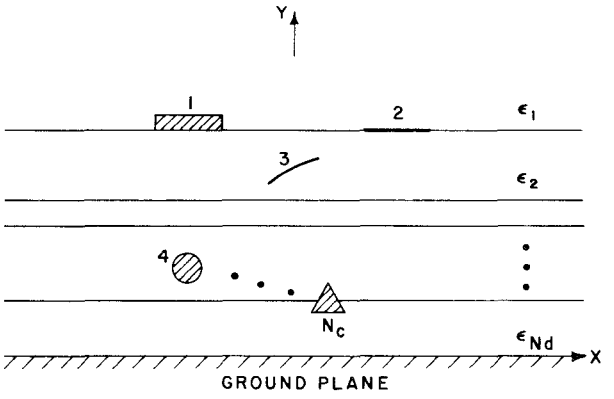

Fig. 1. A multiconductor transmission line in a multilayered dielectric region above a ground plane.

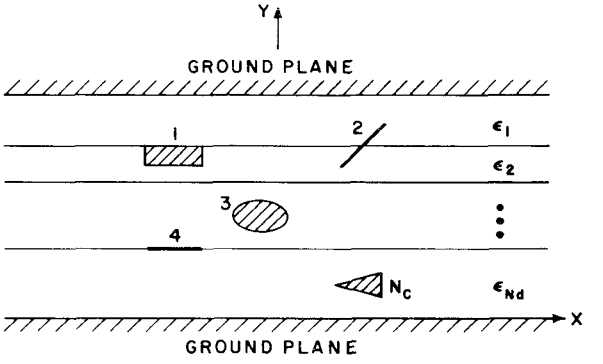

Fig. 2. A multiconductor transmission line in a multilayered dielectric region between two ground planes.

Once the capacitance and inductance matrices of the multiconductor transmission-line system are known, the complete behavior of the system can be determined, to the transmission-line approximation, by multiconductor transmission-line theory [20].

III. Analysis

Consider the capacitance matrix for the problem stated in the previous section. The ijth element of this matrix is the free charge per unit length of surface on the ith conductor when all conductors except the jth conductor are grounded and the jth conductor is charged to a potential of one volt. Hence, the elements of the capacitance matrix can be determined by relating the free charge per unit length of surface on the conductors to the potentials

of the conductors. The free charge per unit length of surface on one of the N_c conductors is the integral of the free charge per unit area over the intersection of the surface of the conductor with the xy plane. Thus, the elements of the capacitance matrix can easily be determined once a relationship has been established between the free charge per unit area on the surfaces of the conductors and the potentials of the conductors.

A total charge σ_T per unit area is assumed on the conductor-to-dielectric interfaces and the N_d-1 dielectric-to-dielectric interfaces. The conductor-to-dielectric interfaces consist of the surfaces of the N_c conductors and the upper ground plane, if present. The jth dielectric-to-dielectric interface is the plane of constant y where the dielectric layers ϵ_j and ϵ_{j+1} meet, provided that no conductors lie on this plane. If conductors lie on this plane, then the jth dielectric-to-dielectric interface is the portion of this plane not occupied by conductors. On each conductor-to-dielectric interface, total charge is the sum of free charge and polarization charge. On each dielectric-to-dielectric interface, total charge is polarization charge. In Section IV, the total charge on the upper ground plane, if present, and the dielectric-to-dielectric interfaces is truncated at a finite negative value of x and a finite positive value of x.

At any point $\underline{\rho}$ in the xy plane and above the lower ground plane, the potential ϕ is due to the combination of σ_T and the image of σ_T about the lower ground plane. Hence

$$\phi(\underline{\rho})=\frac{1}{2\pi\epsilon_0}\sum_{j=1}^{J}\int_{l_j}\sigma_T(\underline{\rho}')\ln\left(\frac{|\underline{\rho}-\hat{\underline{\rho}}'|}{|\underline{\rho}-\underline{\rho}'|}\right)dl' \tag{1}$$

where l_j is the contour of the jth interface in the xy plane. The first N_c interfaces are the surfaces of the N_c conductors. If there is no upper ground plane, the next N_d-1 interfaces are the dielectric-to-dielectric interfaces. If there is an upper ground plane, the (N_c+1)th interface is the surface of this ground plane, and the next N_d-1 interfaces are the dielectric-to-dielectric interfaces. Accordingly

$$J=J_1+J_2 \tag{2}$$

where, in the absence of the upper ground plane

$$\begin{aligned}J_1&=N_c\\ J_2&=N_d-1\end{aligned} \tag{3}$$

and, in the presence of the upper ground plane

$$\begin{aligned}J_1&=N_c+1\\ J_2&=N_d-1.\end{aligned} \tag{4}$$

It is evident that J_1 is the number of conductor-to-dielectric interfaces and that J_2 is the number of dielectric-to-dielectric interfaces. In (1), dl' is the differential element of length at $\underline{\rho}'$ on l_j, and $\hat{\underline{\rho}}'$ is the image of $\underline{\rho}'$ about the lower ground plane.

The electric field $\underline{E}$ is given by

$$\underline{E}(\underline{\rho})=-\underline{\nabla}\phi(\underline{\rho}). \tag{5}$$

Substituting (1) for ϕ in (5), and assuming that $\underline{\rho}$ is not on any of the interfaces $\{l_j\}$ so that the $\underline{\nabla}$ operator may be taken under the integral sign, we obtain

$$\underline{E}(\underline{\rho})=\frac{1}{2\pi\epsilon_0}\sum_{j=1}^{J}\int_{l_j}\sigma_T(\underline{\rho}')\left(\frac{\underline{\rho}-\underline{\rho}'}{|\underline{\rho}-\underline{\rho}'|^2}-\frac{\underline{\rho}-\hat{\underline{\rho}}'}{|\underline{\rho}-\hat{\underline{\rho}}'|^2}\right)dl'. \tag{6}$$

Taking the limit of (6) as $\underline{\rho}$ approaches the interface l_i, we obtain the following formula for $\underline{E}$ valid on l_i:

$$\left[\underline{E}^{\pm}(\underline{\rho})=\frac{1}{2\pi\epsilon_0}\sum_{j=1}^{J}\oint_{l_j}\sigma_T(\underline{\rho}')\left(\frac{\underline{\rho}-\underline{\rho}'}{|\underline{\rho}-\underline{\rho}'|^2}-\frac{\underline{\rho}-\hat{\underline{\rho}}'}{|\underline{\rho}-\hat{\underline{\rho}}'|^2}\right)dl' \pm\underline{n}\frac{\sigma_T(\underline{\rho})}{2\epsilon_0},\quad \begin{cases}\underline{\rho} & \text{on } l_i\\ i=1,2,\cdots J\end{cases}\right] \tag{7}$$

Here, $\underline{n}$ is the unit vector normal to l_i at $\underline{\rho}$. The side of l_i toward which $\underline{n}$ points is called the positive side of l_i. The side of l_i away from which $\underline{n}$ points is called the negative side of l_i. In (7), $\underline{E}^+(\underline{\rho})$ is the electric field on the positive side of l_i, and $\underline{E}^-(\underline{\rho})$ is the electric field on the negative side of l_i. In (7), $\oint_{l_j}$ denotes the principal value of the integral over l_j.

On each conductor-to-dielectric interface, the potential is constant. Denoting the potential on the ith conductor-to-dielectric interface by V_i, we obtain

$$\phi(\underline{\rho})=V_i,\qquad \begin{cases}\underline{\rho} & \text{on } l_i\\ i=1,2,\cdots J_1\end{cases}. \tag{8}$$

If the upper ground plane is present, then V_i is zero for $i=J_1$. Substitution of (1) for $\phi(\underline{\rho})$ in (8) yields

$$\frac{1}{2\pi\epsilon_0}\sum_{j=1}^{J}\int_{l_j}\sigma_T(\underline{\rho}')\ln\left(\frac{|\underline{\rho}-\hat{\underline{\rho}}'|}{|\underline{\rho}-\underline{\rho}'|}\right)dl'=V_i,\quad \begin{cases}\underline{\rho} & \text{on } l_i\\ i=1,2\cdots J_1\end{cases}. \tag{9}$$

The displacement vector is called $\underline{D}(\underline{\rho})$. The y component of $\underline{D}(\underline{\rho})$ is continuous across each dielectric-to-dielectric interface. Since $\underline{D}(\underline{\rho})$ is the product of permittivity with electric field, it follows that

$$\epsilon_{i-J_1}\underline{E}^+(\underline{\rho})\cdot\underline{u}_y=\epsilon_{i+1-J_1}\underline{E}^-(\underline{\rho})\cdot\underline{u}_y,\qquad \begin{cases}\underline{\rho} & \text{on } l_i\\ i=J_1+1,J_1+2,\cdots J\end{cases} \tag{10}$$

where $\underline{u}_y$ is the unit vector in the y direction. In Figs. 1 and 2, the y direction is upward. In (10), ϵ_{i-J_1} and $\underline{E}^+(\underline{\rho})$ are, respectively, the permittivity and electric field on the upper side of l_i. Moreover, ϵ_{i+1-J_1} and $\underline{E}^-(\underline{\rho})$ are, respectively, the permittivity and electric field on the lower side of l_i. Substitution of (7) for $\underline{E}^{\pm}(\underline{\rho})$ in (10) yields, after division by $(\epsilon_{i-J_1}-\epsilon_{i+1-J_1})$

$$\frac{(\epsilon_{i-J_1}+\epsilon_{i+1-J_1})}{2\epsilon_0(\epsilon_{i-J_1}-\epsilon_{i+1-J_1})}\sigma_T(\underline{\rho})+\frac{1}{2\pi\epsilon_0}\sum_{j=1}^{J}\oint_{l_j}\sigma_T(\underline{\rho}')\left(\frac{\underline{\rho}-\underline{\rho}'}{|\underline{\rho}-\underline{\rho}'|^2}-\frac{\underline{\rho}-\hat{\underline{\rho}}'}{|\underline{\rho}-\hat{\underline{\rho}}'|^2}\right)\cdot\underline{u}_y\,dl'=0,\qquad \begin{cases}\underline{\rho} & \text{on } l_i\\ i=J_1+1,J_1+2,\cdots J\end{cases} \tag{11}$$

Equations (9) and (11) are a set of J integral equations in the unknown total charge σ_T per unit area on the interfaces whose contours are $\{l_j, j=1,2,\cdots J\}$. In Section IV, the method of moments will be used to obtain an approximate numerical solution for σ_T in terms of $\{V_i, i=1,2,\cdots N_c\}$. Since (9) and (11) are linear, this solution is of the form

$$\sigma_T = \sum_{i=1}^{N_c} \sigma_T^{(i)} V_i \tag{12}$$

where $\sigma_T^{(i)}$ is the solution which would result if the potential V_i was unity and all other potentials were zero.

As stated earlier, some of the conductors may be of finite cross section, and others may be infinitesimally thin strips. If the ith conductor is of finite cross section, then l_i is a closed curve. On this ith conductor

$$\sigma_T = \epsilon_0 \underline{E} \cdot \underline{n} \tag{13}$$

$$\sigma_F = \epsilon \underline{E} \cdot \underline{n} \tag{14}$$

where $\underline{E}$ is the electric field just outside the conductor, $\underline{n}$ is the unit normal vector which points outward from the surface of the conductor, ϵ is the permittivity just outside the conductor, and σ_F is the free charge per unit area on the conductor. Equations (13) and (14) imply that

$$\sigma_F(\underline{\rho}) = \frac{\epsilon(\underline{\rho})}{\epsilon_0} \sigma_T(\underline{\rho}) \tag{15}$$

on the surface of the ith conductor provided that this conductor is of finite cross section.

If the ith conductor is an infinitesimally thin strip, then l_i runs from one edge of the strip to the other. The free charge σ_F per unit area on the surface of the ith conductor is then given by

$$\sigma_F = (\epsilon^+ \underline{E}^+ - \epsilon^- \underline{E}^-) \cdot \underline{n} \tag{16}$$

where $\underline{n}$ is a unit vector normal to the strip. The side of the strip toward which $\underline{n}$ points is called the positive side. The side of the strip away from which n points is called the negative side. In (16), ϵ^+ and $\underline{E}^+$ are, respectively, the permittivity and electric field on the positive side of the strip. Moreover, ϵ^- and $\underline{E}^-$ are, respectively, the permittivity and electric field on the negative side of the strip. Substitution of (7) for $\underline{E}^{\pm}$ in (16) leads to

$$\sigma_F(\underline{\rho}) = \frac{\epsilon^+(\underline{\rho}) + \epsilon^-(\underline{\rho})}{2\epsilon_0} \sigma_T(\underline{\rho}) + \frac{\epsilon^+(\underline{\rho}) - \epsilon^-(\underline{\rho})}{2\pi\epsilon_0} \cdot \sum_{j=1}^{J} \int_{l_j} \sigma_T(\underline{\rho}') \left(\frac{\underline{\rho} - \underline{\rho}'}{|\underline{\rho} - \underline{\rho}'|^2} - \frac{\underline{\rho} - \hat{\underline{\rho}}'}{|\underline{\rho} - \hat{\underline{\rho}}'|^2} \right) \cdot \underline{n}\, dl' \tag{17}$$

on the surface of the ith conductor, provided that this conductor is an infinitesimally thin strip.

Regardless of whether the ith conductor has finite cross section or is an infinitesimally thin strip, the free charge Q_i per unit length on it is given by

$$Q_i = \int_{l_i} \sigma_F(\underline{\rho})\, dl, \qquad i=1,2,\cdots N_c \tag{18}$$

where dl is the differential element of length at $\underline{\rho}$ on l_i. In view of (12) with the index i replaced by j, substitution of (15) or (17) for σ_F in (18) gives

$$Q_i = \sum_{j=1}^{N_c} C_{ij} V_j, \qquad i=1,2,\cdots N_c \tag{19}$$

where, if the ith conductor is of finite cross section

$$C_{ij} = \int_{l_i} \frac{\epsilon(\underline{\rho})}{\epsilon_0} \sigma_T^{(j)}(\underline{\rho})\, dl. \tag{20}$$

If the ith conductor is an infinitesimally thin strip, then

$$C_{ij} = \int_{l_i} \left\{ \frac{\epsilon^+(\underline{\rho}) + \epsilon^-(\underline{\rho})}{2\epsilon_0} \sigma_T^{(j)}(\underline{\rho}) + \frac{\epsilon^+(\underline{\rho}) - \epsilon^-(\underline{\rho})}{2\pi\epsilon_0} \cdot \sum_{k=1}^{J} \int_{l_k} \sigma_T^{(j)}(\underline{\rho}') \left(\frac{\underline{\rho} - \underline{\rho}'}{|\underline{\rho} - \underline{\rho}'|^2} - \frac{\underline{\rho} - \hat{\underline{\rho}}'}{|\underline{\rho} - \hat{\underline{\rho}}'|^2} \right) \cdot \underline{n}\, dl' \right\} dl. \tag{21}$$

In obtaining (21), the index j in (17) was replaced by k in order to avoid confusion with the index j which appears in C_{ij}. The coefficient C_{ij} is the ijth element of the capacitance matrix.

The inductance matrix is called L. The ijth element of L is the magnetic flux passing between a unit length of the ith conductor and the lower ground plane when one ampere of net z-directed electric current flows on the jth conductor and there is no net z-directed electric current on any of the other conductors. Here, z is the coordinate perpendicular to the xy plane. It is shown in the Appendix that

$$L = \mu_0 \epsilon_0 [C_0]^{-1} \tag{22}$$

where C_0 is the capacitance matrix which would result if all dielectric layers were replaced by free space.

IV. Development of the Moment Solution

In this section, the integral equations (9) and (11) are solved numerically for σ_T by means of the method of moments [21].

A solution σ_T to (9) and (11) is sought in the form

$$\sigma_T(\underline{\rho}) = \sum_{n=1}^{N} \sigma_{Tn} P_n(\underline{\rho}) \tag{23}$$

where $\{P_n(\underline{\rho}), n=1,2,\cdots N\}$ are unit pulse functions which cover $\{l_j, j=1,2,\cdots J\}$. Moreover, $\{\sigma_{Tn}, n=1,2,\cdots N\}$ are constants to be determined. The upper ground plane and dielectric layers are now truncated at a finite negative value of x and a finite positive value of x so that only pulse functions of finite domain are needed.

Given an arbitrary point on the truncated $\{l_j, j=1,2,\cdots J\}$, there is an integer m such that, at this point

$$P_m = 1$$
$$P_n = 0, \qquad n=1,2,\cdots m-1, m+1,\cdots N. \tag{24}$$

It follows from (23) and (24) that

$$\sigma_T = \sigma_{Tm} \tag{25}$$

at this point.

Let $\{P_n(\underline{\rho}), n=1,2,\cdots N_1\}$ be the pulses on $\{l_j, j=1,2,\cdots J_1\}$, and let $\{P_n(\underline{\rho}), n=N_1+1, N_1+2,\cdots N\}$ be the pulses on $\{l_j, j=J_1+1, J_1+2,\cdots, J\}$. Moreover, let $\underline{\rho}_m$ be the midpoint of the domain of $P_m(\underline{\rho})$ for $m=1,2,\cdots N$.

Substituting (23) for σ_T in (9) and then enforcing (9) at $\underline{\rho}=\underline{\rho}_m$ for $m=1,2,\cdots N_1$, we obtain

$$\sum_{n=1}^{N} S_{mn}\sigma_{Tn} = V_i, \qquad m=1,2,\cdots N_1 \tag{26}$$

where i is such that $\underline{\rho}_m$ is on l_i, and

$$S_{mn} = \frac{1}{2\pi\epsilon_0}\int_{\Delta l_n} \ln\left(\frac{|\underline{\rho}_m - \hat{\underline{\rho}}'|}{|\underline{\rho}_m - \underline{\rho}'|}\right) dl', \qquad \begin{cases} m=1,2,\cdots N_1 \\ n=1,2,\cdots N \end{cases} \tag{27}$$

where Δl_n is the domain of $P_n(\underline{\rho})$.

Substituting (23) for σ_T in (11) and then enforcing (11) at $\underline{\rho}=\underline{\rho}_m$ for $m=N_1+1, N_1+2,\cdots N$, we obtain

$$\sum_{n=1}^{N} S_{mn}\sigma_{Tn} = 0, \qquad m=N_1+1, N_1+2,\cdots N \tag{28}$$

where, for $m \neq n$

$$S_{mn} = \frac{1}{2\pi\epsilon_0}\int_{\Delta l_n}\left(\frac{\underline{\rho}_m - \underline{\rho}'}{|\underline{\rho}_m - \underline{\rho}'|^2} - \frac{\underline{\rho}_m - \hat{\underline{\rho}}'}{|\underline{\rho}_m - \hat{\underline{\rho}}'|^2}\right)\cdot \underline{u}_y\, dl', \qquad \begin{cases} m=N_1+1, N_1+2;\cdots N \\ n=1,2,\cdots N \end{cases} \tag{29}$$

In (28), S_{mm} is given by

$$S_{mm} = \frac{\epsilon_{i-J_1}+\epsilon_{i+1-J_1}}{2\epsilon_0(\epsilon_{i-J_1}-\epsilon_{i+1-J_1})} + \frac{1}{2\pi\epsilon_0}\int_{\Delta l_m}\left(\frac{\underline{\rho}_m - \underline{\rho}'}{|\underline{\rho}_m - \underline{\rho}'|^2}\right)\cdot \underline{u}_y\, dl'$$
$$- \frac{1}{2\pi\epsilon_0}\int_{\Delta l_m}\left(\frac{\underline{\rho}_m - \hat{\underline{\rho}}'}{|\underline{\rho}_m - \hat{\underline{\rho}}'|^2}\right)\cdot \underline{u}_y\, dl',$$
$$m = N_1+1, N_1+2,\cdots N. \tag{30}$$

In (30), i is such that $\underline{\rho}_m$ is on Δl_i. If $m \neq n$, but if $\underline{\rho}_m$ and P_n are on the same dielectric-to-dielectric interface, then (29) reduces to

$$S_{mn} = -\frac{1}{2\pi\epsilon_0}\int_{\Delta l_n}\left(\frac{\underline{\rho}_m - \hat{\underline{\rho}}'}{|\underline{\rho}_m - \hat{\underline{\rho}}'|^2}\right)\cdot \underline{u}_y\, dl'. \tag{31}$$

Formulas for calculating S_{mn} are given later in this section. After S_{mn} has been calculated for $m=1,2,\cdots N$ and $n=1,2,\cdots N$, (26) and (28) combine to form N simultaneous equations in the N unknowns $\{\sigma_{Tn}, n=1,2,\cdots N\}$. These simultaneous equations can then be solved for $\{\sigma_{Tn}, n=1,2,\cdots N\}$ in terms of $\{V_i, i=1,2,\cdots N_c\}$. The solution is of the form

$$\sigma_{Tn} = \sum_{i=1}^{N_c} \sigma_{Tn}^{(i)} V_i \tag{32}$$

where $\{\sigma_{Tn}^{(i)}, n=1,2,\cdots N\}$ is the solution which would result if V_i were unity and all other V's were zero. Substituting (32) into (23) and comparing the result with (12), we obtain

$$\sigma_T^{(i)}(\underline{\rho}) = \sum_{n=1}^{N} \sigma_{Tn}^{(i)} P_n(\underline{\rho}). \tag{33}$$

The elements of the capacitance matrix can be calculated by replacing i by j in (33) and then substituting the resulting expression for $\sigma_T^{(j)}(\underline{\rho})$ in (20) and (21). The integral with respect to l in (21) is approximated by sampling the integrand at $\underline{\rho}=\underline{\rho}_m$ for all values of m for which $\underline{\rho}_m$ is on l_i. At $\underline{\rho}=\underline{\rho}_m$, the integrals with respect to l' in (21) are similar to the integrals appearing in expressions (29) and (30) for S_{mn}.

To facilitate calculation of S_{mn}, Δl_n is approximated by the straight line segment shown in Fig. 3. This segment is of length Δ_n and makes an angle θ_n with the x axis. The midpoint of this segment is $\underline{\rho}_n$. Now

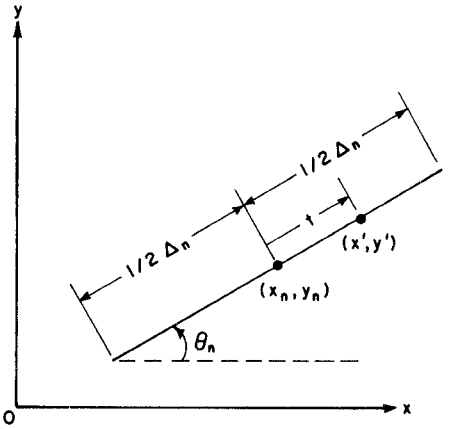

Fig. 3. The straight line segment Δl_n with length Δ_n, midpoint (x_n, y_n), and orientation θ_n.

$$\underline{\rho}_n = \underline{u}_x x_n + \underline{u}_y y_n \tag{34}$$

where $\underline{u}_x$ is the unit vector in the x direction, and x_n and y_n are, respectively, the x and y coordinates of $\underline{\rho}_n$. Similarly, the vectors $\underline{\rho}'$ and $\hat{\underline{\rho}}'$ in expression (27) for S_{mn} are written in terms of their rectangular coordinates as

$$\underline{\rho}' = \underline{u}_x x' + \underline{u}_y y' \tag{35}$$

$$\hat{\underline{\rho}}' = \underline{u}_x x' - \underline{u}_y y'. \tag{36}$$

As can be seen from Fig. 3

$$x' = x_n + t\cos\theta_n \tag{37}$$

$$y' = y_n + t\sin\theta_n. \tag{38}$$

Due to the equations of the previous paragraph, (27) becomes

$$S_{mn} = \frac{1}{4\pi\epsilon_0}\int_{-(1/2)\Delta_n}^{(1/2)\Delta_n} \ln\left(\frac{(x_m - x')^2 + (y_m + y')^2}{(x_m - x')^2 + (y_m - y')^2}\right) dt, \quad \begin{cases} m = 1,2,\cdots N_1 \\ n = 1,2,\cdots N \end{cases} \tag{39}$$

where x' and y' are given by (37) and (38), respectively. After substitution of (37) and (38) for x' and y', (39) reduces to

$$S_{mn} = F_1(a_1, b_1) - F_1(a_2, b_2), \quad \begin{cases} m = 1,2,\cdots N_1 \\ n = 1,2,\cdots N \end{cases} \tag{40}$$

where

$$a_1 = (x_m - x_n)\sin\theta_n + (y_m + y_n)\cos\theta_n \tag{41}$$

$$b_1 = (x_m - x_n)\cos\theta_n - (y_m + y_n)\sin\theta_n \tag{42}$$

$$a_2 = (x_m - x_n)\sin\theta_n - (y_m - y_n)\cos\theta_n \tag{43}$$

$$b_2 = (x_m - x_n)\cos\theta_n + (y_m - y_n)\sin\theta_n \tag{44}$$

and

$$F_1(a, b) = \frac{1}{4\pi\epsilon_0}\int_{-(1/2)\Delta_n - b}^{(1/2)\Delta_n - b} \ln(t^2 + a^2)\, dt. \tag{45}$$

Application of [22, formula 623.] to (45) gives

$$F_1(a, b) = \frac{1}{4\pi\epsilon_0}\left[t\ln(t^2 + a^2) - 2t + 2a\tan^{-1}\left(\frac{t}{a}\right)\right]_{t=-1/2\Delta_n - b}^{t=1/2\Delta_n - b}. \tag{46}$$

If a is zero, then the $\tan^{-1}$ term should be omitted from (46).

Expressions (29) and (30) become

$$S_{mn} = \frac{1}{2\pi\epsilon_0}(I_{mn} - \hat{I}_{mn}), \quad m \neq n, \quad \begin{cases} m = N_1 + 1, N_1 + 2, \cdots N \\ n = 1,2,\cdots N \end{cases} \tag{47}$$

$$S_{mm} = \frac{\epsilon_{l-J_1} + \epsilon_{l+1-J_1}}{2\epsilon_0(\epsilon_{l-J_1} - \epsilon_{l+1-J_1})} - \frac{1}{2\pi\epsilon_0}\hat{I}_{mm}, \quad m = N_1 + 1, N_1 + 2, \cdots N. \tag{48}$$

The first integral in (30) has vanished because Δl_m is a straight line segment. In (48), i is such that $\underline{\rho}_m$ is on l_i. In (47) and (48)

$$I_{mn} = \int_{\Delta l_n}\left(\frac{\underline{\rho}_m - \underline{\rho}'}{|\underline{\rho}_m - \underline{\rho}'|^2}\right)\cdot\underline{u}_y\, dl' \tag{49}$$

and

$$\hat{I}_{mn} = \int_{\Delta l_n}\left(\frac{\underline{\rho}_m - \hat{\underline{\rho}}'}{|\underline{\rho}_m - \hat{\underline{\rho}}'|^2}\right)\cdot\underline{u}_y\, dl'. \tag{50}$$

In the domain of integration of (49), $\underline{\rho}'$ is never equal to $\underline{\rho}_m$, and in (50), $\hat{\underline{\rho}}'$ is never equal to $\underline{\rho}_m$. Hence, the integrands in (49) and (50) are always finite.

Equations (34)–(36) reduce (49) and (50) to

$$I_{mn} = \int_{-1/2\Delta_n}^{1/2\Delta_n} \frac{y_m - y'}{(x_m - x')^2 + (y_m - y')^2}\, dt \tag{51}$$

$$\hat{I}_{mn} = \int_{-1/2\Delta_n}^{1/2\Delta_n} \frac{y_m + y'}{(x_m - x')^2 + (y_m + y')^2}\, dt. \tag{52}$$

Substitution of (37) and (38) for x' and y' in (51) and (52) produces

$$I_{mn} = (y_m - y_n - b_2\sin\theta_n)F_2(a_2, b_2) - (\sin\theta_n)F_3(a_2, b_2) \tag{53}$$

$$\hat{I}_{mn} = (y_m + y_n + b_1\sin\theta_n)F_2(a_1, b_1) + (\sin\theta_n)F_3(a_1, b_1) \tag{54}$$

where a_1, b_1, a_2, and b_2 are given by (41)–(44). Moreover

$$F_2(a, b) = \int_{-1/2\Delta_n - b}^{1/2\Delta_n - b} \frac{dt}{t^2 + a^2} \tag{55}$$

and

$$F_3(a, b) = \int_{-(1/2)\Delta_n - b}^{(1/2)\Delta_n - b} \frac{t\, dt}{t^2 + a^2}. \tag{56}$$

If $a = 0$, then, as is evident from the statement just after (50), t is never zero during the integration in (55). Hence, it is easy to obtain

$$F_2(a, b) = -\left[\frac{1}{t}\right]_{-1/2\Delta_n - b}^{1/2\Delta_n - b}, \quad a = 0 \tag{57}$$

which reduces to

$$F_2(a, b) = \frac{\Delta_n}{b^2 - \frac{1}{4}\Delta_n^2}, \quad a = 0. \tag{58}$$

If $a \neq 0$, application of [22, formula 120.1.] to (55) gives

$$F_2(a, b) = \left[\frac{1}{a}\tan^{-1}\left(\frac{t}{a}\right)\right]_{-1/2\Delta_n - b}^{1/2\Delta_n - b}, \quad a \neq 0. \tag{59}$$

It is evident from the statement just after (50) that $(t^2 + a^2)$ is never zero during the integration in (56). Hence, we easily obtain

$$F_3(a, b) = \frac{1}{2}\left[\ln(t^2 + a^2)\right]_{-1/2\Delta_n - b}^{1/2\Delta_n - b} \tag{60}$$

which is valid regardless of the value of a.

V. Numerical Examples

A computer program has been written for the special case where all conductors are of finite cross section and for the case where all conductors are infinitesimally thin [23]. This program was used to obtain the results given in this section. These results agree well with those of various references.

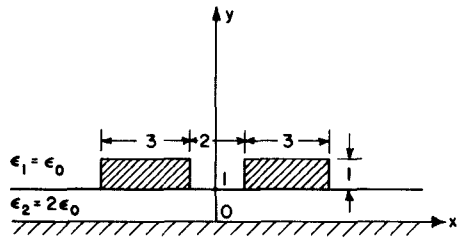

Fig. 4. Coupled microstrips.

TABLE I
COMPARISON OF RESULTS FOR THE COUPLED MICROSTRIP IN FIG. 4. UNITS ARE F/m

	Our Results	Reference [11]	Reference [3]
C_{11}	0.9165×10^{-10}	0.9017×10^{-10}	0.9224×10^{-10}
C_{12}	-0.8220×10^{-11}	-0.8059×10^{-11}	-0.8504×10^{-11}
C_{21}	-0.8220×10^{-11}	-0.8059×10^{-11}	-0.8504×10^{-11}
C_{22}	0.9165×10^{-10}	0.9017×10^{-10}	0.9224×10^{-10}

Example 1

Consider the pair of coupled microstrips touching a dielectric slab over a conducting plane as shown in Fig. 4. The left-hand conductor is conductor 1. The right-hand conductor is conductor 2. Table I compares our computed results with those of [3] and [11]. For comparison, the results of [3] have been changed to farads per meter. For our results, we used 16 subsections on each conductor, and on the dielectric interface we used 10 subsections from -9 to -4, 4 subsections from -1 to $+1$, and 10 subsections from 4 to 9. The difference between our results and those of [3] is less than 4 percent. The difference between our results and those of [11] is less than 2 percent. The difference should become smaller as we increase the number of our subsections.

Example 2

Consider two conductors in two different dielectric layers above a ground plane as shown in Fig. 5. The left-hand conductor is conductor 1. The right-hand conductor is conductor 2. The number of subsections used on conductor 1 is 6, the number on conductor 2 is 6, and the number on the dielectric interface is 16 extending from $x = -0.8$ to $x = +0.8$. In Table II, our results are compared with those obtained by using the computer program of [11]. The agreement is excellent in all cases. In the table, C_{ij} is the ijth element of the capacitance matrix, C_{0ij} is the ijth element of the free-space capacitance matrix, and L_{ij} is the ijth element of the inductance matrix.

Example 3

Here, the two conductors of the transmission line are located in the same dielectric layer, as shown in Fig. 6. The left-hand conductor is conductor 1. The right-hand conductor is conductor 2. The number of subsections used on conductor 1 is 6, the number on conductor 2 is 6, and the number used on the dielectric interface is 16 extending

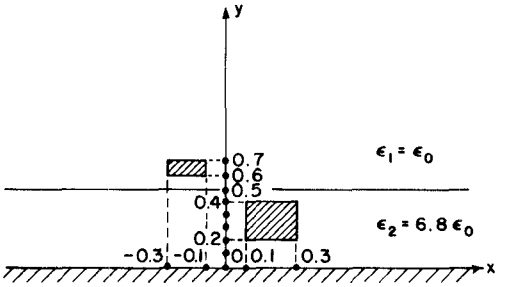

Fig. 5. Two conductors in two different dielectric layers.

TABLE II
COMPARISON OF RESULTS FOR EXAMPLE 2, FIG. 5. CAPACITANCE IS IN F/m. INDUCTANCE IS IN H/m

	Our Results	Reference [11]
C_{11}	0.3651×10^{-10}	0.3701×10^{-10}
C_{12}	-0.1562×10^{-10}	-0.1520×10^{-10}
C_{21}	-0.1562×10^{-10}	-0.1523×10^{-10}
C_{22}	0.2099×10^{-9}	0.2108×10^{-9}
C_{011}	0.2296×10^{-10}	0.2296×10^{-10}
C_{012}	-0.8808×10^{-11}	-0.8805×10^{-11}
C_{021}	-0.8808×10^{-11}	-0.8810×10^{-11}
C_{022}	0.3772×10^{-10}	0.3772×10^{-10}
L_{11}	0.5315×10^{-6}	0.5403×10^{-6}
L_{12}	0.1241×10^{-6}	0.1229×10^{-6}
L_{21}	0.1241×10^{-6}	0.1265×10^{-6}
L_{22}	0.3235×10^{-6}	0.3204×10^{-6}

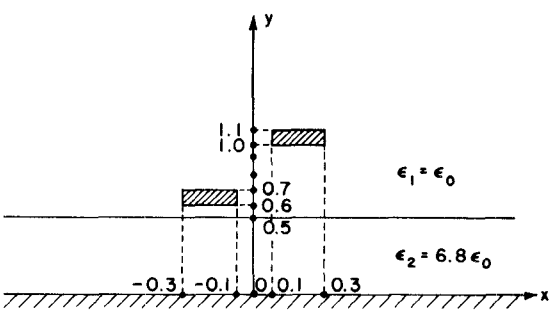

Fig. 6. Two conductors in the same dielectric layer.

TABLE III
COMPARISON OF RESULTS FOR EXAMPLE 3, FIG. 6. CAPACITANCE IS IN F/m. INDUCTANCE IS IN H/m

	Our Results	Reference [11]
C_{11}	0.3720×10^{-10}	0.3757×10^{-10}
C_{12}	-0.6889×10^{-11}	-0.6657×10^{-11}
C_{21}	-0.6889×10^{-11}	-0.6597×10^{-11}
C_{22}	0.2169×10^{-10}	0.2217×10^{-10}
C_{011}	0.2391×10^{-10}	0.2391×10^{-10}
C_{012}	-0.8427×10^{-11}	-0.8427×10^{-11}
C_{021}	-0.8427×10^{-11}	-0.8427×10^{-11}
C_{022}	0.2042×10^{-10}	0.2042×10^{-10}
L_{11}	0.5437×10^{-6}	0.5501×10^{-6}
L_{12}	0.2244×10^{-6}	0.2235×10^{-6}
L_{21}	0.2244×10^{-6}	0.2292×10^{-6}
L_{22}	0.6368×10^{-6}	0.6407×10^{-6}

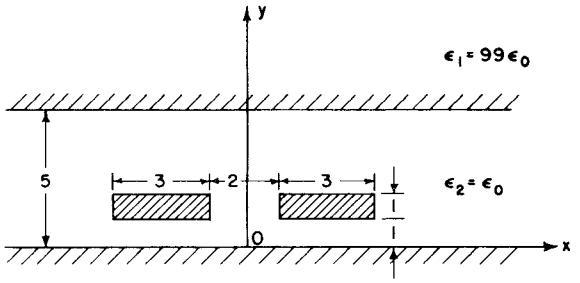

Fig. 7. Coupled microstrips between parallel conducting planes.

TABLE IV
COMPARISON OF RESULTS FOR EXAMPLE 4, FIG 7. UNITS ARE F/m

	Results obtained by using $\epsilon_1 = 99\epsilon_0$	Results obtained by truncating the upper ground plane	Reference [3]
C_{11}	0.6233×10^{-10}	0.6264×10^{-10}	0.6307×10^{-10}
C_{12}	-0.5931×10^{-11}	-0.5724×10^{-11}	-0.5866×10^{-11}
C_{21}	-0.5931×10^{-11}	-0.5724×10^{-11}	-0.5866×10^{-11}
C_{22}	0.6233×10^{-10}	0.6264×10^{-10}	0.6307×10^{-10}

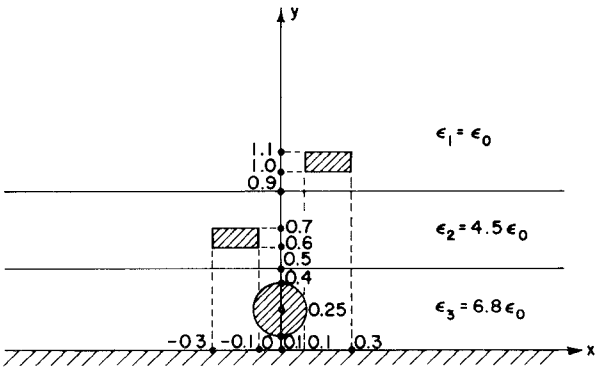

Fig. 8. Three conductors in three different dielectric layers.

TABLE V
RESULTS FOR EXAMPLE 5, FIG. 8. CAPACITANCE IS IN F/m. INDUCTANCE IS IN H/m

i	j	C_{ij}	C_{0ij}	L_{ij}
1	1	0.1244×10^{-9}	0.2828×10^{-10}	0.4965×10^{-6}
1	2	-0.1300×10^{-10}	-0.7678×10^{-11}	0.1996×10^{-6}
1	3	-0.6825×10^{-10}	-0.1181×10^{-10}	0.1183×10^{-6}
2	1	-0.1300×10^{-10}	-0.7678×10^{-11}	0.1996×10^{-6}
2	2	0.3340×10^{-10}	0.2090×10^{-10}	0.6163×10^{-6}
2	3	-0.7196×10^{-11}	-0.3030×10^{-11}	0.7728×10^{-6}
3	1	-0.6825×10^{-10}	-0.1181×10^{-10}	0.1183×10^{-6}
3	2	-0.7196×10^{-11}	-0.3030×10^{-11}	0.7728×10^{-6}
3	3	0.3523×10^{-9}	0.5468×10^{-10}	0.2331×10^{-6}

from $x = -0.8$ to $x = +0.8$. In Table III, our results are compared with those obtained by using the computer program of [11]. The agreement is excellent.

Example 4

Fig. 7 shows an example with two ground planes. The left-hand conductor is conductor 1. The right-hand conductor is conductor 2. The approach taken in this paper is to truncate the upper ground plane at a finite width. Another approach is to replace the upper ground plane with a dielectric layer of permittivity $\epsilon_1 \gg \epsilon_2$ as discussed in [11]. Results are compared in Table IV.

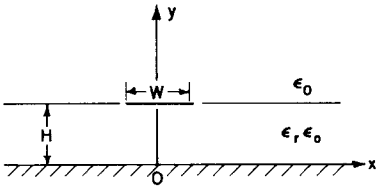

Fig 9. A microstrip line.

TABLE VI
CHARACTERISTIC IMPEDANCES Z_0 IN OHMS FOR EXAMPLE 6, FIG. 9

	$\varepsilon_r = 6.0$			$\varepsilon_r = 9.5$		
W/H	Our results	Reference [4]	Reference [13]	Our results	Reference [4]	Reference [13]
0.4	92.2785	91.172	89.909	74.8970	73.702	73.290
0.7	73.9626	73.613	71.995	59.9105	59.379	58.502
1.0	62.8109	62.713	60.970	50.8097	50.501	49.431
2.0	42.9980	43.149	41.510	34.6743	34.592	33.493
4.0	26.9709	27.301	26.027	21.6679	21.763	20.906
10.0	12.9961	13.341	12.485	10.3940	10.568	9.981

Example 5

This example consists of three conducting lines in three dielectric layers as shown in Fig. 8. The left-hand conductor is conductor 1, the right-hand conductor is conductor 2, and the cylinder is conductor 3. We used 12 subsections on conductors 1 and 2, 8 subsections on conductor 3, and 20 subsections on each dielectric interface. Our computed results are listed in Table V. No other results are available for comparison.

Example 6

Consider a single microstrip with zero thickness on a dielectric substrate above a conducting plane as shown in Fig. 9. The characteristic impedance Z_0 of the microstrip is [2]

$$Z_0 = \frac{1}{v_0\sqrt{CC_0}} \tag{61}$$

where v_0 is the velocity of light in free space, C is the capacitance of the microstrip, and C_0 is the free-space capacitance of the microstrip. For various ratios W/H, Table VI compares our results for Z_0 with those of [4] and [13]. The results attributed to [13] appear in [4] and were calculated from [13, eq. (1)], which is based on curves obtained from Wheeler's conformal mapping analysis [12]. Our results were obtained by using 12 subsections on the strip, 15 on the part of the dielectric interface from $-2W$

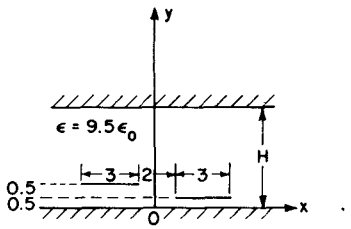

Fig. 10. Two coupled microstrip lines between two ground planes.

TABLE VII
COMPARISON OF RESULTS FOR EXAMPLE 7, FIG. 10. CAPACITANCE IS IN F/m. INDUCTANCE IS IN H/m. ZERO-THICKNESS RESULTS ARE DENOTED BY *. NONZERO-THICKNESS RESULTS ARE DENOTED BY Δ

H	3		5	
	*	Δ	*	Δ
C_{11}	0.5356×10^{-9}	0.5394×10^{-9}	0.4852×10^{-9}	0.4884×10^{-9}
C_{12}	-0.9250×10^{-11}	-0.9547×10^{-11}	-0.1798×10^{-10}	-0.1841×10^{-10}
C_{21}	-0.9250×10^{-11}	-0.9547×10^{-11}	-0.1798×10^{-10}	-0.1841×10^{-10}
C_{22}	0.7834×10^{-9}	0.7895×10^{-9}	0.7557×10^{-9}	0.7615×10^{-9}
C_{011}	0.5466×10^{-10}	0.5504×10^{-10}	0.4951×10^{-10}	0.4984×10^{-10}
C_{012}	-0.9439×10^{-12}	-0.9742×10^{-12}	-0.1835×10^{-11}	-0.1879×10^{-11}
C_{021}	-0.9439×10^{-12}	-0.9742×10^{-12}	-0.1835×10^{-11}	-0.1879×10^{-11}
C_{022}	0.7994×10^{-10}	0.8056×10^{-10}	0.7712×10^{-10}	0.7770×10^{-10}
L_{11}	0.2033×10^{-6}	0.2019×10^{-6}	0.2246×10^{-6}	0.2231×10^{-6}
L_{12}	0.2401×10^{-8}	0.2442×10^{-8}	0.5345×10^{-8}	0.5396×10^{-8}
L_{21}	0.2401×10^{-8}	0.2442×10^{-8}	0.5345×10^{-8}	0.5396×10^{-8}
L_{22}	0.1390×10^{-6}	0.1380×10^{-6}	0.1442×10^{-6}	0.1431×10^{-6}

to $-W/2$, and 15 on the part of the dielectric interface from $W/2$ to $2W$.

Example 7

Consider the two coupled microstrips between two ground planes shown in Fig. 10. The left-hand strip is conductor 1. The right-hand strip is conductor 2. Both strips are infinitesimally thin. Parameters can be calculated directly for the zero-thickness strips. Alternatively, the zero-thickness strips can be approximated by strips having a small but nonzero thickness. Table VII compares the zero-thickness results with the nonzero-thickness results for $H = 3$ and $H = 5$. These results were obtained by using 10 subsections on each zero-thickness strip, 22 subsections on each nonzero-thickness strip, and 36 subsections on the upper ground plane from -9 to $+9$. The nonzero-thickness strips are 0.001 thick.

Example 8

Consider three infinitesimally thin strips embedded in a three-layered dielectric between two ground planes as shown in Fig. 11. The left-hand strip is conductor 1, the right-hand strip is conductor 2, and the center strip is conductor 3. Our computed results are listed in Table VIII. No other results are available for comparison. Our results were obtained by using 6 subsections on each strip, 38 subsections on each dielectric interface, and 38 subsections on the upper ground plane.

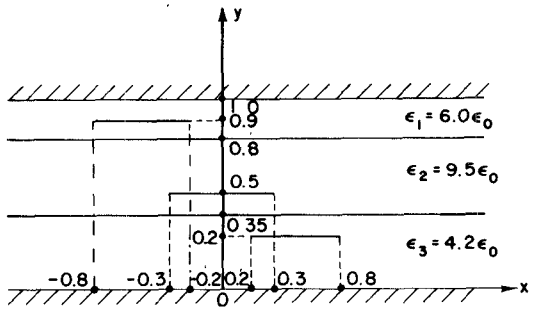

Fig. 11. Three striplines in a three-layered dielectric between two ground planes.

TABLE VIII
RESULTS FOR EXAMPLE 8, FIG. 11. CAPACITANCE IS IN F/m. INDUCTANCE IS IN H/m

i	j	C_{ij}	C_{oij}	L_{ij}
1	1	0.4900×10^{-9}	0.7773×10^{-10}	0.1456×10^{-6}
1	2	-0.5737×10^{-12}	-0.1036×10^{-12}	0.5630×10^{-8}
1	3	-0.6457×10^{-10}	-0.7193×10^{-11}	0.2844×10^{-7}
2	1	-0.5737×10^{-12}	-0.1036×10^{-12}	0.5630×10^{-8}
2	2	0.2459×10^{-9}	0.5212×10^{-10}	0.2240×10^{-6}
2	3	-0.6138×10^{-10}	-0.9788×10^{-11}	0.5762×10^{-7}
3	1	-0.6457×10^{-10}	-0.7193×10^{-11}	0.2844×10^{-7}
3	2	-0.6137×10^{-10}	-0.9788×10^{-11}	0.5762×10^{-7}
3	3	0.2865×10^{-9}	0.3876×10^{-10}	0.3065×10^{-6}

VI. DISCUSSION AND CONCLUSION

The integral equations (9) and (11) for the total charge at the surfaces of the conducting transmission lines, at the upper ground plane, and on the dielectric-to-dielectric interfaces are simple in concept. Their solution by the method of moments using pulse functions for expansion and point matching for testing is also simple. Experience has shown that this type of solution is both versatile and accurate. Improvement in the rate of convergence might be obtained by using better behaved functions for expansion and testing, but at the cost of considerable complication.

The solution is valid for an arbitrary number of conductors and an arbitrary number of dielectric layers. It is valid if a conductor touches a dielectric interface, straddles a dielectric interface, or is totally within one dielectric region. Theoretically, the solution is valid if some conductors are infinitesimally thin and others are of finite cross section. However, the computer program of [23] was not written to include the case where both infinitesimally thin conductors and finite cross-section conductors are present.

Theoretically, the upper ground plane and the dielectric interfaces are infinitely wide. However, the numerical solution is obtained by truncating them at a finite width. From computational experience, it appears that the numerical solution will be sufficiently accurate if they are truncated at a width equal to two or three times the transverse extent of the conducting transmission lines.

The solution can be easily extended to multilayered magnetic media by the concept of duality [24, sec. 3-2].

However, this extension is seldom of practical interest and is not considered here.

It should be remembered that the basic formulation is exact only in the limit as the frequency approaches zero. At high frequencies, the true solution is not a transverse electromagnetic wave, but is a hybrid one. In other words, the true solution is not obtained by solving Laplace's equation, but rather by solving a coupled wave equation. This solution is extremely complicated, and experience indicates that the transverse electromagnetic wave approximation is sufficiently accurate for most purposes.

Appendix

Relationship (22) exists between the inductance matrix and the free-space capacitance matrix of a multiconductor transmission line. Since we could not find a general proof of (22) in the literature, we give one here.

Consider the magnetostatic problem in which a specified amperage of steady z-directed electric current is forced to flow on each of the N_c conductors of either Fig. 1 or Fig. 2 where the permeability of each dielectric layer is μ_0. It is assumed that the electric current flows only in the z direction. The specified electric current will distribute itself over the surface of each of the N_c conductors, and surface densities of z-directed electric current will be induced on the ground plane(s) so that the normal component of magnetic field is zero on each of the N_c conductors and the ground plane(s). The surfaces of the N_c conductors are called the first N_c interfaces. If there is an upper ground plane, its surface is called the (N_c+1)th interface.

Let S_i be the surface bounded by a z-directed line from $z=0$ to $z=1$ on the ith interface, a z-directed line from $z=0$ to $z=1$ on the lower ground plane, and connections in the $z=0$ and $z=1$ planes. The magnetic flux ψ_i passing through S_i is given by

$$\psi_i = \iint_{S_i} \underline{B}\cdot d\underline{s} = \iint_{C_i} \underline{A}\cdot d\underline{l} = A_{z_i}. \tag{A1}$$

In (A1), C_i is the contour that bounds S_i, $\underline{B}$ is the magnetic field, $\underline{A}$ is the magnetic vector potential, and A_{z_i} is the z component of the magnetic vector potential on the line where S_i meets the ith interface. It has been assumed that the z component of the magnetic vector potential vanishes on the lower ground plane. Since the normal component of magnetic field is zero on the ith interface, ψ_i does not depend on the placement of the line where S_i meets the ith interface. It is now evident from (A1) that

$$A_z(\underline{\rho}) = \psi_i \tag{A2}$$

where $A_z(\underline{\rho})$ is the z component of magnetic vector potential at an arbitrary point $\underline{\rho}$ on the ith interface, and ψ_i is a constant flux. Equation (A2) annihilates the normal component of magnetic field on the surface of the ith interface.

Using image currents to annihilate the normal component of magnetic field on the lower ground plane, we write $A_z(\underline{\rho})$ as

$$A_z(\underline{\rho}) = \frac{\mu_0}{2\pi}\sum_{k=1}^{J_1}\int_{l_k} J_z(\underline{\rho}')\ln\left(\frac{|\underline{\rho}-\hat{\underline{\rho}}'|}{|\underline{\rho}-\underline{\rho}'|}\right)dl' \tag{A3}$$

where J_1 is given by either (3) or (4). Furthermore, $J_z(\underline{\rho}')$ is the z component of electric current per unit length on the J_1 interfaces, $\underline{\rho}'$ is the point at which the differential element of length dl' is located, and $\hat{\underline{\rho}}'$ is the image of $\underline{\rho}'$ about the lower ground plane. Substitution of (A3) into (A2) yields the magnetostatic equation

$$\frac{\mu_0}{2\pi}\sum_{k=1}^{J_1}\int_{l_k} J_z(\underline{\rho}')\ln\left(\frac{|\underline{\rho}-\hat{\underline{\rho}}'|}{|\underline{\rho}-\underline{\rho}'|}\right)dl' = \psi_i, \qquad \begin{cases}\underline{\rho} & \text{on } l_i\\ i=1,2,\cdots J_1\end{cases}. \tag{A4}$$

Consider the electrostatic equations (9) and (11). If all dielectric layers are replaced by free space, the total charge density σ_T reduces to the free charge density σ_F. Consequently, the electrostatic equation (9) becomes

$$\frac{1}{2\pi\epsilon_0}\sum_{j=1}^{J_1}\int_{l_j}\sigma_F(\underline{\rho}')\ln\left(\frac{|\underline{\rho}-\hat{\underline{\rho}}'|}{|\underline{\rho}-\underline{\rho}'|}\right)dl' = V_i, \quad \begin{cases}\underline{\rho} & \text{on } l_i\\ i=1,2,\cdots J_1\end{cases}. \tag{A5}$$

Furthermore, the electrostatic equation (11) disappears.

The solution $J_z(\underline{\rho}')$ to (A4) is of the form

$$J_z(\underline{\rho}') = \sum_{i=1}^{N_c} J_z^{(i)}(\underline{\rho}')\psi_i \tag{A6}$$

where $J_z^{(i)}(\underline{\rho}')$ is the solution that would result if $\psi_i=1$ and all other ψ's were zero. In (A6), the index i terminates at N_c because, if there is an upper ground plane, then it has been assumed that the z component of the magnetic vector potential vanishes on it so that ψ_{N_c+1} is zero. The solution $\sigma_F(\underline{\rho}')$ to (A5) is of the form

$$\sigma_F(\underline{\rho}') = \sum_{i=1}^{N_c}\sigma_F^{(i)}(\underline{\rho}')V_i \tag{A7}$$

where $\sigma_F^{(i)}(\underline{\rho}')$ is the solution which would result if $V_i=1$ and all other V's were zero. In (A7), the index i terminates at N_c because the upper ground plane, if present, is at zero potential. It is evident from (A4) and (A5) that

$$J_z^{(i)}(\underline{\rho}') = \frac{1}{\mu_0\epsilon_0}\sigma_F^{(i)}(\underline{\rho}'). \tag{A8}$$

Substitution of (A8) into (A6) gives

$$J_z(\underline{\rho}') = \frac{1}{\mu_0\epsilon_0}\sum_{i=1}^{N_c}\sigma_F^{(i)}(\underline{\rho}')\psi_i. \tag{A9}$$

The integral over l_j of (A7) is

$$Q_j = \sum_{i=1}^{N_c} C_{oji}V_i, \qquad j=1,2,\cdots N_c \tag{A10}$$

where Q_j is the free charge per unit length on the jth conductor and C_{oji} is the jith element of the free-space capacitance matrix.

$$C_{oji} = \int_{l_j}\sigma_F^{(i)}(\underline{\rho}')\,dl', \qquad \begin{cases}i=1,2,\cdots N_c\\ j=1,2,\cdots N_c\end{cases}. \tag{A11}$$

The integral over l_j of (A9) is

$$I_j = \frac{1}{\mu_0\epsilon_0}\sum_{i=1}^{N_c} C_{oji}\psi_i, \qquad j=1,2,\cdots N_c \tag{A12}$$

where I_j is the net z-directed electric current on the jth conductor and C_{0ji} is given by (A11).

Solving (A12) for the ψ's in terms of the I's, we obtain

$$\psi_i = \mu_0 \epsilon_0 \sum_{j=1}^{N_c} [C_0]_{ij}^{-1} I_j \qquad \text{(A13)}$$

where $[C_0]_{ij}^{-1}$ is the ijth element of the inverse of the free-space capacitance matrix. This inverse exists because the free-space capacitance matrix C_0 is positive definite. In view of the definition of the inductance matrix L, the desired relationship (22) between L and C_0 is evident from (A13).

REFERENCES

[1] P. Silvester, "TEM wave properties of microstrip transmission lines," *Proc. Inst. Elec. Eng.*, vol. 115, pp. 43–48, Jan. 1968.

[2] T. G. Bryant and J. A. Weiss, "Parameters of microstrip transmission lines and of coupled pairs of microstrip lines," *IEEE Trans. Microwave Theory Tech.*, vol. MTT-16, pp. 1021–1027, Dec. 1968.

[3] W. T. Weeks, "Calculation of coefficients of capacitance of multiconductor transmission lines in the presence of a dielectric interface," *IEEE Trans. Microwave Theory Tech.*, vol. MTT-18, pp. 35–43, Jan. 1970.

[4] A. Farrar and A. T. Adams, "Characteristic impedance of microstrip by the method of moments," *IEEE Trans. Microwave Theory Tech.*, vol. MTT-18, pp. 65–66, Jan. 1970.

[5] E. Yamashita and K. Atsuki, "Strip line with rectangular outer conductor and three dielectric layers," *IEEE Trans. Microwave Theory Tech.*, vol. MTT-18, pp. 238–244, May 1970.

[6] J. L. Allen and M. F. Estes, "Broadside-coupled strips in a layered dielectric medium," *IEEE Trans. Microwave Theory Tech.*, vol. MTT-20, pp. 662–669, Oct. 1972.

[7] J. L. Allen, "Odd and even mode capacitances for coupled strips in a layered medium," *Int. J. Electron.*, vol. 35, pp. 1–13, July 1973.

[8] A. Farrar and A. T. Adams, "Multilayer microstrip transmission lines," *IEEE Trans. Microwave Theory Tech.*, vol. MTT-22, pp. 889–891, Oct. 1974.

[9] R. Crampagne, M. Ahmadpanah, and J. Guiraud, "A simple method for determining the Green's function for a large class of MIC lines having multilayered dielectric structures," *IEEE Trans. Microwave Theory Tech.*, vol. MTT-26, pp. 82–87, Feb. 1978.

[10] C. E. Smith and R. S. Chang, "Microstrip transmission line with finite-width dielectric," *IEEE Trans. Microwave Theory Tech.*, vol. MTT-28, pp. 90–94, Feb. 1980.

[11] C. Wei and R. F. Harrington, "Computation of the parameters of multiconductor transmission lines in two dielectric layers above a ground plane," Depart. Electrical Computer Eng., Syracuse Univer., Rep. TR-82-12, Nov. 1982.

[12] H. A. Wheeler, "Transmission-line properties of parallel strips separated by a dielectric sheet," *IEEE Trans. Microwave Theory Tech.*, vol. MTT-13, pp. 172–185, Mar. 1965.

[13] H. Sobol, "Extending IC technology to microwave equipment," *Electronics*, vol. 40, pp. 112–124, Mar. 20, 1967.

[14] E. Yamashita, "Variational method for the analysis of microstrip-like transmission lines," *IEEE Trans. Microwave Theory Tech.*, vol. MTT-16, pp. 529–535, Aug. 1968.

[15] R. Mittra and T. Itoh, "Charge and potential distributions in shielded striplines," *IEEE Trans. Microwave Theory Tech.*, vol. MTT-18, pp. 149–156, Mar. 1970.

[16] A. Farrar and A. T. Adams, "Computation of propagation constants for the fundamental and higher order modes in microstrip," *IEEE Trans. Microwave Theory Tech.*, vol. MTT-24, pp. 456–460, July 1976.

[17] T. Itoh and A. S. Hebert, "A generalized spectral domain analysis for coupled suspended microstriplines with tuning septums," *IEEE Trans. Microwave Theory Tech.*, vol. MTT-26, pp. 820–826, Oct. 1978.

[18] T. Itoh, "Generalized spectral domain method for multiconductor printed lines and its application to turnable suspended microstrips," *IEEE Trans. Microwave Theory Tech.*, vol. MTT-26, pp. 983–987, Dec. 1978.

[19] R. Plonsey and R. E. Collin, *Principles and Applications of Electromagnetic Fields*. New York: McGraw-Hill, 1961.

[20] D. Kajfez, "Multiconductor transmission lines," Depart. Electrical Eng., Univ. Mississippi, June 1972. Also published as Interaction Note 151 by Dr. Carl Baum, Air Force Weapons Laboratory (EL), Kirtland AFB, NM 87117.

[21] R. F. Harrington, *Field Computation by Moment Methods*. New York: Macmillan Co., 1968. Reprinted by Krieger Publishing Co., Melbourne, FL, 1982.

[22] H. B. Dwight, *Tables of Integrals and Other Mathematical Data*, Fourth Ed. New York: Macmillan Co., 1961.

[23] C. Wei and R. F. Harrington, "Extension of the multiconductor transmission line solution to zero-thickness conductors and to conductors between parallel ground planes," Depart. Electrical Computer Eng., Syracuse Univer., Rep. TR-83-5, Mar. 1983.

[24] R. F. Harrington, *Time-Harmonic Electromagnetic Fields*. New York: McGraw-Hill, 1961.

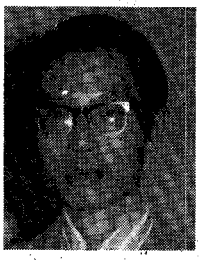

Cao Wei was born in Changsha, Hunan Province, China, in 1939. He graduated and received the B.S. degree from the Beijing Institute of Posts and Telecommunications in 1959.

After graduation, he taught mathematics for three years in the Nanjing Institute of Posts and Telecommunications, Nanjing, China. He then returned to the Beijing Institute of Posts and Telecommunications to study in the Department of Radio Telecommunication, from which he graduated in 1965. Since then, he has taught and done research in the areas of electromagnetics, microwave techniques, and antennas at the Nanjing Institute of Posts and Telecommunications. In September 1981, he came to the United States as a Visiting Scholar to undertake research with Prof. R. F. Harrington in the Department of Electrical and Computer Engineering, Syracuse University.

Roger F. Harrington (S'48–A'53–M'57–SM'62–F'68) was born in Buffalo, NY, on December 24, 1925. He received the B.E.E. and M.E.E. degrees from Syracuse University, Syracuse, NY, in 1948 and 1950, respectively, and the Ph.D. degree from Ohio State University, Columbus, OH, in 1952.

From 1945 to 1946, he served as an Instructor at the U.S. Naval Radio Materiel School, Dearborn, MI, and from 1948 to 1950, he was employed as an Instructor and Research Assistant at Syracuse University. While studying at Ohio State University, he served as a Research Fellow in the Antenna Laboratory. Since 1952, he has been on the faculty of Syracuse University, where he is presently Professor of Electrical Engineering. During 1959–1960 he was Visiting Associate Professor at the University of Illinois, Urbana, in 1964 he was Visiting Professor at the University of California, Berkeley, and in 1969 he was Guest Professor at the Technical University of Denmark, Lyngby, Denmark.

Dr. Harrington is a member of Tau Beta Pi, Sigma Xi, and the American Association of University Professors.

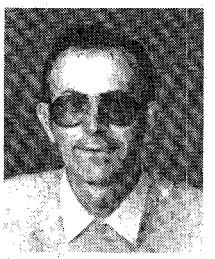

Joseph R. Mautz (S'66–M'67–SM'75) was born in Syracuse, NY, on April 29, 1939. He received the B.S., M.S., and Ph.D degrees in electrical engineering from Syracuse University, Syracuse, NY, in 1961, 1965, and 1969, respectively.

He is a Research Engineer in the Department of Electrical Engineering, Syracuse University, working on radiation and scattering problems. His primary fields of interest are electromagnetic theory and applied mathematics. He is currently working in the area of numerical methods for solving field problems.

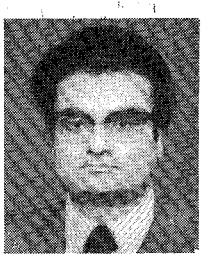

Tapan K. Sarkar (S'69–M'76–SM'81) was born in Calcutta, India, on August 2, 1948. He received the B.Tech. degree from the Indian Institute of Technology, Kharagpur, India, in 1969, the M.Sc.E. degree from the University of New Brunswick, Fredericton, Canada, in 1971, and the M.S. and Ph.D. degrees from Syracuse University, Syracuse, NY, in 1975.

From 1969 to 1971, he served as an Instructor at the University of New Brunswick. While studying at Syracuse University, he served as an Instructor and Research Assistant in the Department of Electrical and Computer Engineering, where he is presently an Adjunct Assistant Professor. Since 1976, he has been an Assistant Professor at the Rochester Institute of Technology, Rochester, NY. From 1977 to 1978, he was a Research Fellow at the Gordon McKay Laboratory of Harvard University, Cambridge, MA. His current research interests deal with system identification, signal processing, and analysis of electrically large electromagnetic systems.

Dr. Sarkar is a member of Sigma Xi and URSI Commission B.

Short Papers

Determination of the Characteristic Impedance by a Step Current Density Approximation

STEPHAN A. IVANOV AND GEORGI L. DJANKOV

Abstract—**The step current densities are used to determine the characteristic impedance of a transmission line with rectangular shape of the conductors. Numerical results for different rectangular lines with asymmetrical position of the inner conductor are presented. The comparison of the results for the square and rectangular coaxial lines shows quite good agreement with the known data.**

I. Introduction

The characteristic impedance of the rectangular coaxial transmission line can be determined with good accuracy for all cases of interest [1]. When the axis of the inner and outer conductors does not coincide and their dimensions differ considerably, the problem becomes complicated. A general expression for the characteristic impedance is derived in [2], but no numerical data are given for the line with asymmetrical position of the conductors. Also, a doubly eccentric rectangular line is considered by Chen [3] for the case of a sufficiently small gap between conductors. An analytical expression for the characteristic impedance of the rectangular line with arbitrary dimensions can be found in [4]. Since the impedance in [4] is calculated by the utilization of the mean value current densities, which may differ considerably from the true current distribution on the inner conductor surface, an error of several percent exists. The purpose of the present short paper is to improve the accuracy of the characteristic impedance calculation by using the step current density approximation. In this way, the edge discontinuity of the current distribution is taken into consideration and an error less than one percent for the impedance values can be obtained.

II. Theoretical Results

The investigated rectangular transmission line is shown in Fig. 1. Since the cross section of this line coincides with the single cell of the four-conductor line considered in [4], the characteristic impedance can be determined by the expression (4) in [4]—the case of the odd–odd mode of excitation. Here it is proposed that the current distribution $J_k(1)$ be replaced by a set of step current densities J_{kq}. For the case when the l_k-wall is divided into N_k intervals with a length l_k/N_k, the final result for the characteristic impedance of the investigated line can be expressed by the formula

$$Z\sqrt{\frac{\epsilon_r}{\mu r}} = \frac{120}{\pi^2} \frac{\sum_{i,j=1}^{4} \sum_{q,r=1}^{N_k} J_{iq} J_{jr} \sum_{m=1}^{\infty} \frac{\beta_{irm}\beta_{jrm} Z_{ijqrm}}{m^3(1-e^{-2m\pi B})}}{\left[\sum_{q=1}^{N_{1,2}} (J_{1q}+J_{2q}) \frac{W}{N_{1,2}} + \sum_{q=1}^{N_{3,4}} (J_{3q}+J_{4q}) \frac{T}{N_{3,4}}\right]^2}$$

where

$$\beta_{1rm} = \sin m\pi D \quad \beta_{2rm} = \sin m\pi (D+T)$$

$$\beta_{3rm} = \beta_{4rm} = \cos m\pi \left(D + T\frac{r-1}{N_{3,4}}\right) - \cos m\pi \left(D + T\frac{r}{N_{3,4}}\right).$$

The coefficients $Z_{ijqrm} = Z_{jiqrm}$ are determined as follows:

$$\begin{aligned}
Z_{11qrm} = Z_{12qrm} = Z_{22qrm} &= e^{-m\pi W(q-r+1/N_{1,2})} \\
&\cdot [1 + e^{-2m\pi(B - W(q-r+1/N_{1,2}))}] \\
&+ e^{-m\pi W(q-r-1/N_{1,2})} [1 + e^{-2m\pi(B - W(q-r-1/N_{1,2}))}] \\
&- 2e^{-m\pi W(q-r/N_{1,2})} [1 + e^{-2m\pi(B - W(q-r/N_{1,2}))}] \\
&- (1 - e^{-m\pi(W/N_{1,2})})^2 [e^{-m\pi(2S + W(q+r-2/N_{1,2}))} \\
&+ e^{-m\pi(2B-2S-W(q+r/N_{1,2}))}]
\end{aligned}$$

$$\begin{aligned}
Z_{13qrm} = Z_{23qrm} &= (1 - e^{-(m\pi W/N_{1,2})})(1 - e^{-2m\pi S}) \\
&\cdot [e^{-m\pi W(q-1/N_{1,2})} + e^{-m\pi(2B-2S-W(q/N_{1,2}))}]
\end{aligned}$$

$$Z_{33qrm} = (1 - e^{-2m\pi S})[1 - e^{-2m\pi(B-S-W)}]$$

$$\begin{aligned}
Z_{14qrm} = Z_{24qrm} &= (1 - e^{-(m\pi W/N_{1,2})}) \\
&\cdot [1 - e^{-m\pi(2S + W(2q-1/N_{1,2}))}] \\
&\cdot [e^{-m\pi W(1-(q/N_{1,2}))} - e^{-m\pi(2B-2S-W(1-(q/N_{1,2})))}]
\end{aligned}$$

$$Z_{34qrm} = e^{-m\pi W}(1 - e^{-2m\pi S})[1 - e^{-2m\pi(B-S-W)}]$$

$$Z_{44qrm} = [1 - e^{-2m\pi(S+W)}][1 - e^{-2m\pi(B-S-W)}].$$

Manuscript received March 1, 1983; revised November 14, 1983.

The authors are with the Department of Radiophysics and Electronics, Sofia University, BG-1126 Sofia, Bulgaria.

0018-9480/84/0400-0450$01.00 ©1984 IEEE